



Short communication

Electrochemical performance and thermal cyclicability of industrial-sized anode supported planar solid oxide fuel cells

Jun Luo ^a, Dong Yan ^a, Dawei Fang ^a, Fengli Liang ^b, Jian Pu ^a, Bo Chi ^a, Z.H. Zhu ^b, Jian Li ^{a,*}

^a Center for Fuel Cell Innovations, School of Materials Science and Engineering, State Key Laboratory of Material Processing and Die & Mould Technology, Huazhong University of Science & Technology, Wuhan, Hubei 430074, China

^b Department of Chemical Engineering, University of Queensland, Brisbane, Qld 4072, Australia

HIGHLIGHTS

- Large-scale anode supported planar SOFC cells fabricated by tape casting-screen printing-cofiring process.
- Electrochemical performance and thermal cyclicability evaluated at 750 °C in a single cell stack.
- Issues affecting the performance of large-scale single cell stack discussed.

ARTICLE INFO

Article history:

Received 6 August 2012

Received in revised form

22 September 2012

Accepted 24 September 2012

Available online 29 September 2012

Keywords:

Solid oxide fuel cell

Industrial-sized cell

Electrochemical performance

Thermal cyclicability

ABSTRACT

Industrial-sized planar anode-supported SOFC cells with a cell dimension of $15 \times 15 \times 0.1$ cm and an active area of 13×13 cm 2 are fabricated through a processing route of tape casting-screen printing-cofiring. Electrochemical performance and thermal cyclicability of the cell are evaluated in a single cell stack at 750 °C with H₂ as the fuel and air as the oxidant. With a gas flow rate of 3 L min $^{-1}$, the initial open circuit voltage (OCV) is 1164 mV, and the stack demonstrates a power density of 380 mW cm $^{-2}$ at 473 mA cm $^{-2}$ with an extrapolated maximum power output of 100 W. After three thermal cycles, the reduction of the stack output voltage is around 5%, and the OCV is maintained at a level above 1145 mV. Based on the obtained results, issues related to stack performance, such as cell quality, contact resistance and sealing, are discussed.

© 2012 Elsevier B.V. All rights reserved.

1. Introduction

As a kind of high efficiency and environment friendly energy conversion technology, solid oxide fuel cell (SOFC) has attracted extensive attention for several decades. The high temperature SOFCs are operated at temperatures near 1000 °C, leading to problems in material selection, fabrication and maintenance, which have obstructed the development of SOFC technology [1,2]. Since the end of last century, efforts on lowering SOFC operating temperature to the intermediate range (600–800 °C) have been made by using anode supported planar cells with thin film electrolyte. Different methods have been adopted for preparing thin film electrolyte, including chemical or physical deposition and ceramic powder processes, among which screen-printing is

a promising thin film technology for mass production owing to its low cost and simple processing procedure [3]. Screen-printed electrolyte films were evaluated in SOFCs [4–10], and rather high power density was achieved with button cells. However, total power output of a SOFC cell depends not only on its power density, but also on its active area; therefore cell size scale-up are required for commercialization of SOFC technology.

Blum et al. [11] have realized that cell size is an important feature in characterizing the potential of SOFC technology. Unfortunately, scaling up an anode-supported planar cell is always a huge technical challenge, because there are some associated problems that need to be overcome. Firstly, it is difficult to manufacture an industrial-sized, flat and defect free anode-supported cell with uniform functional electrolyte and electrodes. For example, tape-casting process is used for fabricating the anode support, and screen-printing process is used for fabricating the thin electrodes and electrolyte, then tape-casting, screen-printing and followed sintering processes all need to be carefully controlled to maintain the thickness uniformity and minimize the adverse effect

* Corresponding author. Tel.: +86 27 87557694; fax: +86 27 87558142.

E-mail address: lijian@hust.edu.cn (J. Li).

caused by the mismatch in coefficient of thermal expansion (CTE) between different functional layers. Secondly, in a stack of anode supported planar SOFC cells, issues related to sealing, interface contact and reactant distribution will affect its performance [12]. In the present study, industrial-sized anode supported planar SOFC cells were fabricated and evaluated in single cell stacks in terms of electrochemical performance and thermal cyclicability; and the sealing, interface contact and gas distribution in the stack were also carefully considered.

2. Experimental

2.1. Cell preparation

Tape casting-screen printing and sintering processes were used for fabrication of the industrial-sized anode supported planar SOFC cells; the processing procedure is diagramed in Fig. 1. NiO (Type Standard, Inco) and Y_2O_3 stabilized ZrO_2 (TZ8YS, Tosoh) in 57:43 weight ratio were ball milled for 24 h in toluene and ethanol mixture solvent with added fish oil as the dispersant and corn starch as the pore former. The slurry was further milled for another 24 h after adding polyvinyl butyral as the binder and polyethylene glycol as the plasticizer. Such prepared slurry was cast into sheet (anode support) by using a tape casting machine (LY-250-3, Beijing Oriental Tai Yang Systems, China), and the thickness of the dried green anode support was 1.4 mm. Functional anode (NiO-YSZ, Inco Type F-Tosoh TZ8Y) and cathode (proprietary material HUST-C) as well as electrolyte (TZ8Y, Tosoh) were then screen printed in sequence on the anode support ($18.7 \times 18.7 \text{ cm}^2$), followed by sintering at 1390°C for 3 h under load. The sintered size of the cell was approximately $15 \times 15 \times 1 \text{ cm}$, and the active area of cell was $13 \times 13 \text{ cm}^2$. Fig. 2 shows the appearance (Fig. 2a) and flatness (Fig. 2b) of the cell. In order to achieve a flat and defect free cell, the heating rate was carefully controlled below 2°C min^{-1} before sintering temperature was reached; and the load applied on the cell by a porous

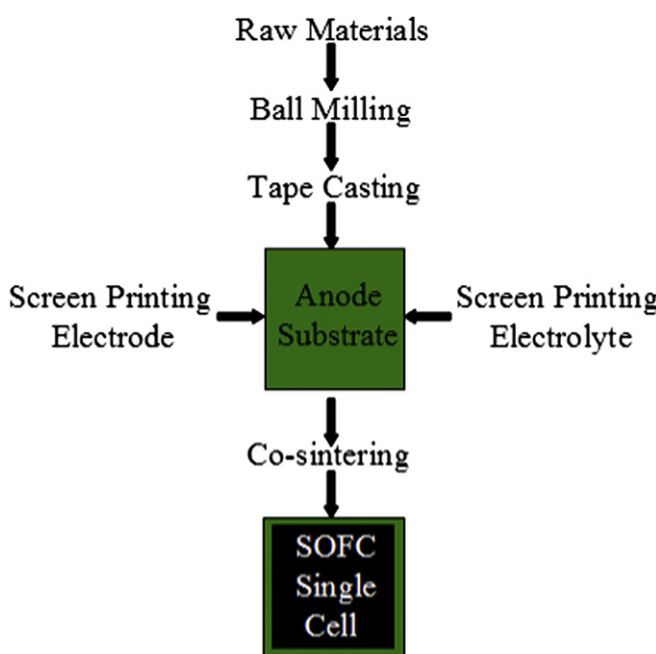


Fig. 1. The processing diagram for fabrication of industrial-sized anode supported SOFC cells.

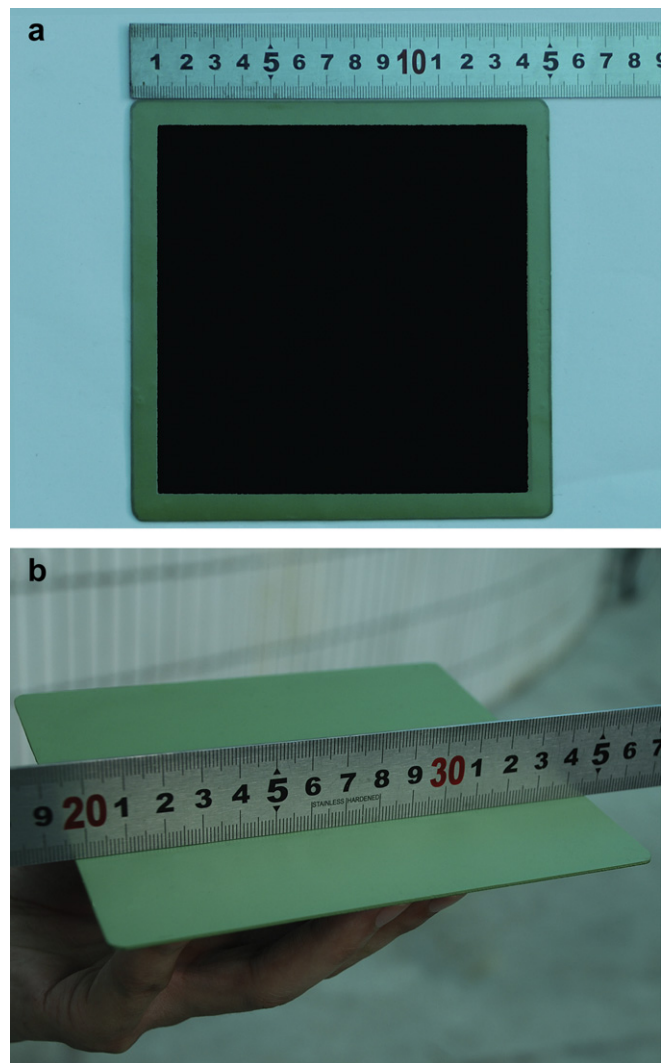


Fig. 2. The appearance (a) and flatness (b) of industrial-sized SOFC cell fabricated by tape casting-screen printing-cofiring process.

ceramic plate during sintering was cautiously adjusted within the range of several grams per square centimeter.

2.2. Electrochemical characterization

Electrochemical performance of the single cell stack was evaluated at SOFC testing station (SF-30, Wuhan Li Xing Testing Equipment). Fig. 3 shows the schematic of the testing setup. The cell was housed by a testing jig, which was made from SUS 430 stainless steel and consisted of the anode and cathode compartments. The fuel gas was distributed to the anode by a piece of Ni foam and air was distributed by ribbed grooves. $\text{LaCo}_{0.6}\text{Ni}_{0.4}\text{O}_3$ (LCN) powder, applied in the form of slurry, was used as the contact layer between the cathode and the grooves to reduce the contact resistance, and the cell was sealed at the periphery on both the anode and cathode sides by compressive sealing components of window-frame shaped mica and glass paste-coated Al_2O_3 tape, respectively. Pure H_2 and dry air were fed at a constant rate of 3 L min^{-1} to the anode and cathode, respectively, as the fuel and oxidant. After a slow startup from room temperature to 750°C , the electrochemical performance and thermal cyclicability of the cell was evaluated.

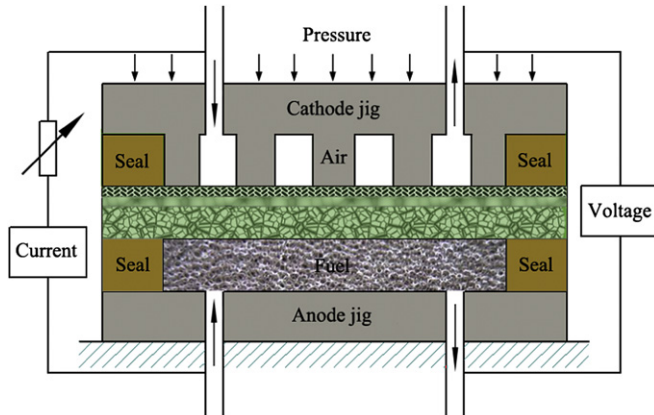


Fig. 3. The schematic setup of the single cell stack for evaluation of electrochemical performance and thermal cycle stability.

3. Result and discussion

3.1. Cell microstructure

Upon startup of the single cell stack test, the microstructure of the anode support and functional anode was evolved with time and temperature. In the sintered cell, they were consisted of NiO and YSZ and gradually reduced to Ni and YSZ in the reduced atmosphere of startup anode gas (5 vol% H₂–N₂ mixture). Such Ni species conversion in the anode support and functional anode generated a significant amount of pores to guarantee fuel gas permeability [13] and triple phase boundaries for electrochemical reaction, and provided excellent electronic conduction [14]. Fig. 4 shows the cross-sectional microstructure of the cell which was kept at 500 °C for 1 h and then continuously heated to 750 °C. The microstructure of the anode support was optimized by adjusting the mass ratio of NiO and YSZ and by introducing pore former [15]. After fully reduced to Ni and YSZ, as confirmed by X-ray diffraction patterns shown in Fig. 5, the porosity of the anode support was

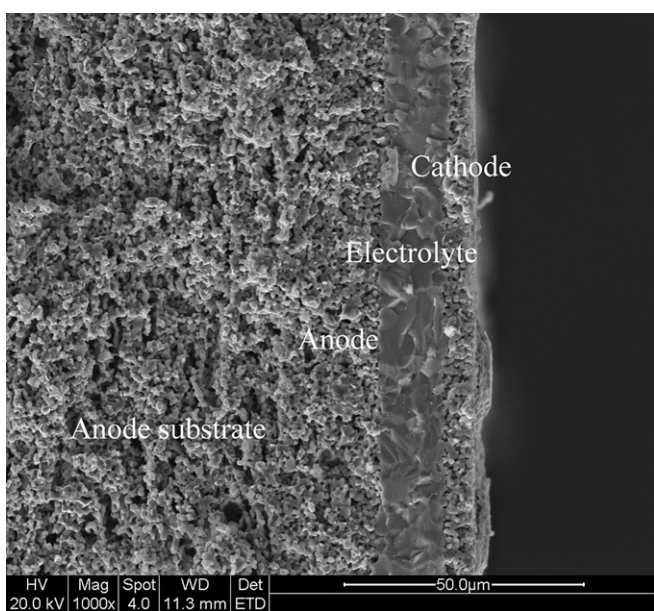


Fig. 4. The cross-sectional microstructure of the industrial-sized anode supported planar cell fully reduced in 5 vol% H₂–N₂ mixture gas.

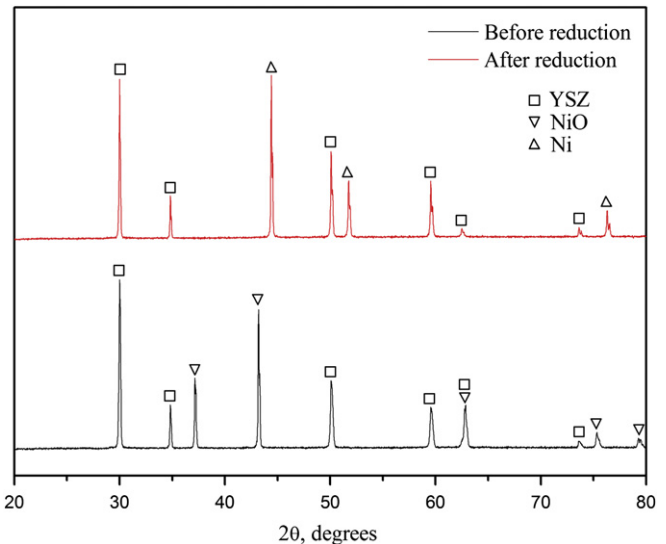


Fig. 5. X-ray diffractions patterns of the NiO–YSZ anode substrate before and after reduction.

around 36%. The functional anode and cathode were well adhered to the electrolyte, with an average thickness of 5 μm, respectively; and the electrolyte layer was dense with an average thickness of 13 μm, guaranteeing a low ohmic resistance at 750 °C.

3.2. Stack performance and thermal cyclicity

Fig. 6 shows the electrochemical performance of a 15 × 15 cm² single cell stack (active area 13 × 13 cm²) at 750 °C with pure H₂ as the fuel and air as the oxidant. Because the highest electrical current that can be supplied by the testing station SF-30 is limited to 80 A, the stack performance at current densities higher than 473 mA cm⁻² could not be characterized, instead extrapolated results up to 1200 mA cm⁻² were included in Fig. 6, according to

$$P_w = I(E_r - R_t I) \quad (1)$$

where P_w is the output power of the cell, I is the current, E_r is the reversible cell voltage, and R_t is the total polarization loss (essentially ohmic loss) [16]. It is seen that a high open circuit voltage of 1164 mV was obtained, which proves that 1) the YSZ electrolyte

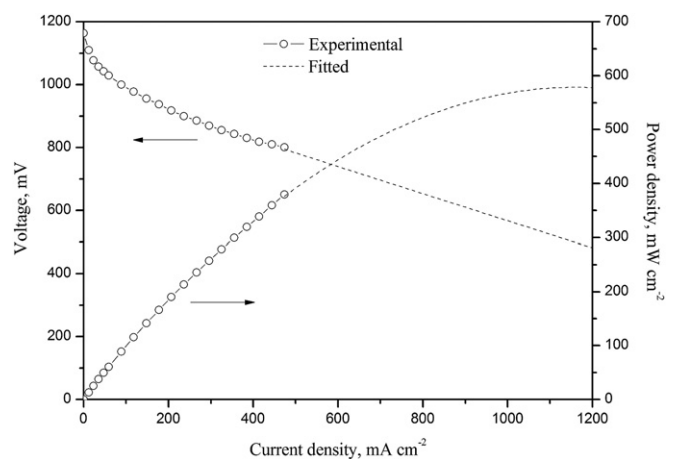


Fig. 6. I–V and power density curves of the single cell stack tested at 750 °C with hydrogen and air as the fuel and oxidant, respectively.

layer was dense, as shown in Fig. 4, without significant gas cross over; and 2) the performance of the sealing components was excellent. In the low current density range below 100 mA cm^{-2} , the non-linear voltage drop was caused by polarization losses of both the anode and cathode, and the approximately linear voltage drop at higher current density was caused by the ohmic loss of the cell, including the resistances mainly contributed by the electrolyte and contact interfaces. According to the extrapolation, the highest power this $15 \times 15 \text{ cm}^2$ cell can offer is around 100 W, which is fairly acceptable for commercial stack applications. Following the initial measurement of current–voltage (I – V) and power curves, the single cell stack was thermal cycled three times between 750 and 300 °C, 750 and 350 °C, and 750 and 400 °C, respectively. After each thermal cycle, it was kept at 240 mA cm^{-2} for endurance evaluation. Fig. 7 shows its thermal cycling performance for over 50 h. Before the first thermal cycle, the OCV was 1180 mV and the stack output voltage at 240 mA cm^{-2} was stabilized at 868 mV. And they decreased, respectively, to 1148 mV and 853 mV after the first thermal cycle, to 1145 mV and 835 mV after the second thermal cycle, and to 1145 mV and 824 mV after the third thermal cycle. The overall decrease in the OCV and stack output voltage after three thermal cycles within 50 h was only 3% and 5%, respectively, which indicates that this single cell stack is thermally cyclical.

3.3. Issues affecting stack performance

There are several issues that can affect the performance of the single cell stack. First of all, it is the quality of the cell, which is characterized by the I – V curve in three distinguishable losses, that is, the non-linear activation loss at low current densities caused by electrodes, the linear ohmic loss at the intermediate current densities primarily contributed by electrolyte and the fast voltage drop at high current densities controlled by mass transport limitation [16]. In the case of the present study at 750 °C, the activation loss occurred approximately at current densities below 100 mA cm^{-2} where with a voltage drop of around 164 mV from 1164 mV to 1000 mV, which is around 14% of the OCV and is quite acceptable for such an industrial-sized planar cell. This is benefited from the highly activated electrodes used in preparing the cell. As estimated from the I – V curve shown in Fig. 6, the area specific ohmic resistance (ASR) of the single cell stack is approximately $430 \text{ m}\Omega \text{ cm}^2$, which includes the contributions mainly from the electrolyte and interfacial contacts. The conductivity of the YSZ used for this cell was measured to be $4.8 \times 10^{-2} \text{ S cm}^{-1}$ [17], which gives a low ASR of $27 \text{ m}\Omega \text{ cm}^2$ for the $13 \mu\text{m}$ thick YSZ electrolytes and suggests that a significant part of the stack ohmic loss was

contributed from the contact materials and interfaces. The mass transport loss is brought about by slow reactant diffusion in electrodes, limiting fuel or air supply for electrochemical reaction. With the cell size scale up, reactant gas distribution becomes one of the most severe problems that affect the cell performance. In the single cell stack test, the fuel was distributed unimpededly to the cell by a piece of 97% porous Ni-foam and further to the functional anode through the 36% porous anode support; and the air was delivered to the cell by ribbed grooves ($1.65 \times 1.0 \text{ mm}$) and then to the cathode through a slurry converted porous layer ($\sim 100 \mu\text{m}$) of LCN contact material. Therefore, similar to the result reported in a previous study [10], the mass transport loss was not an issue for this single cell stack.

As mentioned above, contact resistance contributes to the ohmic loss of the single cell stack. With the increase in cell size, contact issue becomes more critical, especially on the cathode side where porous powdery ceramics are frequently used as the contact material [18–20]. In the present study, Ni-foam and LCN were used as the contact material on the anode and cathode side, respectively. Ni-foam is extremely conductive and its resistance can be neglected compared to other components in the stack. At 750 °C, the conductivity of the LCN is as high as around 1300 S cm^{-1} [18]; and the ASR contributed by a piece of $100 \mu\text{m}$ thick dense LCN is only $7.69 \times 10^{-3} \text{ m}\Omega \text{ cm}^2$. Assuming the dried LCN slurry was 60% porous, and then the calibrated ASR of the LCN contact layer should be $1.28 \times 10^{-2} \text{ m}\Omega \text{ cm}^2$, which is still negligible relative to the measured high ohmic loss ($430 \text{ m}\Omega \text{ cm}^2$) of the single cell stack. Based on this analysis, it can be certain that the contact interfaces on both the cathode and anode sides generate most part of the ohmic loss in the single cell stack. Jiang et al. [21] has proved that contact resistance reduces considerably with the increase of contact area by increasing compressive load. With the cell size increased, the compressive load applied on the stack should be increased accordingly for a better interface contact. It is realized that increasing the stack load will increase the risk of breaking the cell, a balance between applying adequate compressive load and maintaining cell integrity should be reached to minimize the stack ohmic loss. In the present study, the compressive load for the single cell stack test was 0.06 MPa; and it is expected that further

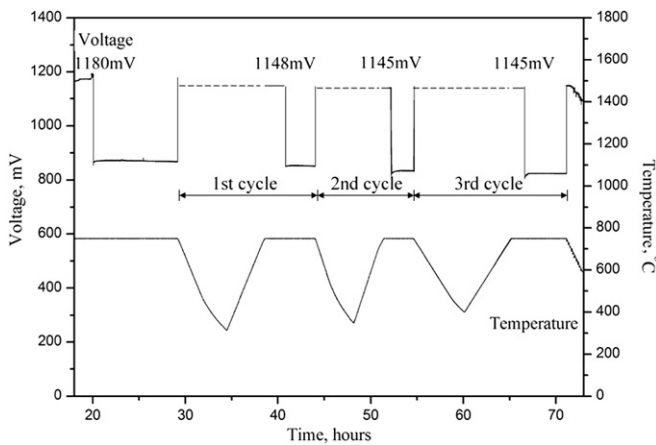


Fig. 7. Thermal cycling performance of the single cell stack.

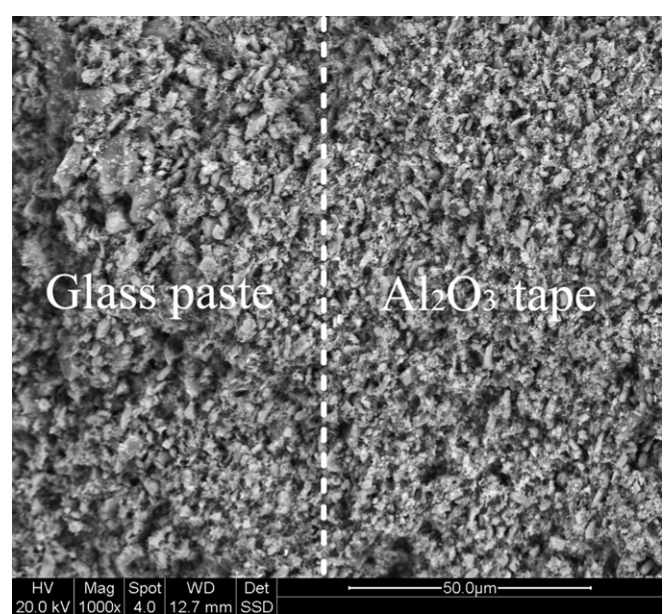


Fig. 8. Interface morphology of glass paste-coated Al_2O_3 tape seal after three thermal cycles.

increasing the compressive load into the range of 0.1 and 0.2 MPa will significantly decrease the stack ohmic loss and in turn improve the stack performance.

One of the major challenges of planar SOFC technology is the need for seals that confine fuel and oxidant gases in the anode and cathode compartments, respectively. The sealing materials are required to be chemically stable in both oxidizing and reducing atmospheres with a CTE closely matched to the cell and interconnect. Various kinds of materials have been developed for the sealing purpose, including glasses, glass-ceramics, ceramics, metal-ceramics and mica [22–24]. In the present test, thin sheet mica and self-developed Al_2O_3 tape seal were used for the cathode and anode compartments, respectively. It is confirmed that the interface are the major leaking channel [25]; therefore, a thin layer of $\text{SiO}_2\text{--MgO}\text{--BaO}\text{--ZnO}\text{--B}_2\text{O}_3$ glass paste was applied on the surface of Al_2O_3 tape to enhance the sealing performance at the interfaces. Under compressive load at 750 °C, the glass was deformable to fully fill the gap between the Al_2O_3 tape seal and the anode support, preventing possible leakage caused by slight warpage of the large cell. Fig. 8 shows the cross-section of the glass paste-coated Al_2O_3 tape seal. The glass was closely adhered to surface of Al_2O_3 tape seal, suggesting there was no appreciable fuel leakage the interface surface. Both anode and cathode seals were kept integral after the test and neither macro breakages nor micro cracks were observed. It is the flexible design of the seal that secured the high initial OCV of 1164 mV and maintained the thermal cycle OCV at the high level above 1145 mV for the large scale single cell stack.

4. Conclusions

Industrial-sized planar anode-supported SOFC cells with a cell dimension of $15 \times 15 \times 0.1$ cm and an active area of $13 \times 13 \text{ cm}^2$ were fabricated through a processing route of tape casting–screen printing–cofiring. Electrochemical performance and thermal cyclicability of the cell were evaluated in a single cell stack at 750 °C, with mica and glass paste-coated Al_2O_3 tape as cathode and anode seals, respectively, and LCN as the contact material. Based on the results, the following conclusions are made.

- 1) The single cell stack has demonstrated outstanding electrochemical performance and thermal cyclicability. The stack power density at 473 mA cm^{-2} is 380 mW cm^{-2} and the extrapolated maximum stack power output can reach 100 W. After three thermal cycles, the stack output voltage drop is around 5%.
- 2) The contribution to the ohmic loss of the single cell stack from the YSZ electrolyte in the cell and the cathode contact material LCN is insignificant; and the contact interfaces generate the majority of the ohmic loss. Therefore, in order to reduce the

ohmic loss in a planar SOFC stack, the applied compressive load needs to be adequate to maintain intimate interface contact without breaking the cells.

- 3) Glass paste-coated Al_2O_3 tape seal has demonstrated excellent sealing performance and thermal cycle stability in the large scale single cell stack. The initial OCV is 1164 mV; and it is maintained at the level above 1145 mV after three thermal cycles with an OCV reduction of 3%.

Acknowledgments

This research was financially supported by the National “863” program (2011AA050702), and Hubei Province Innovation Team Project (2008CDA004). The SEM and XRD characterizations were assisted by the Analytical and Testing Center of Huazhong University of Science and Technology.

References

- [1] J.P.P. Huijsmans, F.P.F. van Berkel, G.M. Christie, *J. Power Sources* 71 (1998) 107–110.
- [2] D.J.L. Brett, A.A. Atkinson, N.P. Brandon, S.J. Skinner, *Chem. Soc. Rev.* 37 (2008) 1568–1578.
- [3] J. Will, A. Mitterdorfer, C. Kleinlogel, D. Perednis, L.J. Gauckler, *Solid State Ionics* 131 (2000) 79–96.
- [4] Y. Matsuzaki, I. Yasuda, *Solid State Ionics* 152–153 (2002) 463–468.
- [5] P.V. Dollen, S. Barnett, *J. Am. Ceram. Soc.* 88 (2005) 3361–3368.
- [6] Y.H. Zhang, X.Q. Huang, Z. Lu, Z.G. Liu, *J. Power Sources* 160 (2006) 1065–1073.
- [7] X.D. Ge, X.Q. Huang, Y.H. Zhang, Z. Lu, *J. Power Sources* 159 (2006) 1048–1050.
- [8] K.J. Yoon, P. Zink, S. Gopalan, U.B. Pal, *J. Power Sources* 172 (2007) 39–49.
- [9] Y.H. Zhang, Z. Lu, X. Huang, M. An, B. Wei, W. Su, *J. Solid State Electrochem.* 15 (2011) 2661–2665.
- [10] J. Wang, D. Yan, J. Pu, B. Chi, J. Li, *Int. J. Hydrog. Energy* 36 (2011) 7234–7239.
- [11] L. Blum, W.A. Meulenberg, H. Nabielek, R.S. Wilckens, *Int. J. Appl. Ceram. Technol.* 2 (2005) 482–492.
- [12] T. Dey, P.C. Ghosh, D. Singdeo, M. Bose, R.N. Basu, *Int. J. Hydrog. Energy* 36 (2011) 9967–9976.
- [13] J.H. Lee, J.W. Heo, D.S. Lee, *Solid State Ionics* 158 (2003) 225–232.
- [14] J.H. Lee, H. Moon, H.W. Lee, J. Kima, J.D. Kima, K.H. Yoon, *Solid State Ionics* 148 (2002) 15–26.
- [15] J.R. Wilson, S.A. Barnett, *Electrochim. Solid State Lett.* 11 (2008) B181–B185.
- [16] N.Q. Minh, T. Takahashi, *Science and Technology of Ceramic Fuel Cells*, Elsevier, Amsterdam, 1995.
- [17] B. Jiang, *Hydrothermal Growth of 8YSZ and Study of its Properties*, M.S. thesis, Huazhong University of Science & Technology, Wuhan, 2008.
- [18] F.Z. Wang, D. Yan, W.Y. Zhang, B. Chi, J. Pu, J. Li, *Int. J. Hydrog. Energy* <http://dx.doi.org/10.1016/j.ijhydene.2012.06.052>.
- [19] S. Sugita, Y. Yoshida, H. Orui, K. Nozawa, M. Arakawa, H. Arai, *J. Power Sources* 185 (2008) 932–936.
- [20] M.C. Tucker, L. Cheng, L.C. DeJonghe, *J. Power Sources* 196 (2011) 8313–8322.
- [21] S.P. Jiang, J.G. Love, L. Apateanu, *Solid State Ionics* 160 (2003) 15–26.
- [22] R.N. Singh, *Int. J. Appl. Ceram. Technol.* 4 (2007) 134–144.
- [23] S.B. Sang, W. Li, J. Pu, J. Li, *J. Power Sources* 177 (2008) 77–82.
- [24] Z. Dai, J. Pu, D. Yan, B. Chi, J. Li, *Int. J. Hydrog. Energy* 36 (2011) 3131–3137.
- [25] S.B. Sang, J. Pu, S.P. Jiang, J. Li, *J. Power Sources* 182 (2008) 141–144.